Dental Research Journal

Original Article

Study esthetic restoration of maxillary central teeth: Optical properties and color coordination in young adults in Isfahan

Ali Raddanipour, Mehrdad Kazemian, Sara Gholizadeh

Department of Operative Dentistry, Dental School, Isf. C., Islamic Azad University, Isfahan, Iran

ABSTRACT

Background: This study investigates the critical role of esthetics in restoring anterior teeth, particularly maxillary central teeth, emphasizing the need for restorations that closely mimic natural tooth appearance. Achieving visual harmony and precise color coordination across all tooth areas is essential, with the opalescent area and halo being vital for maintaining restoration integrity. While previous research has addressed tooth color and opalescent characteristics, this study aims to provide a deeper analysis of their optical properties (L, a, b) among individuals aged 20–30 years in Isfahan, using cross-polarized photography.
Materials and Methods: In this descriptive analytical research involved 191 participants from the Faculty of Dentistry at Islamic Azad University of Isfahan, all without dental abnormalities or prior restorations. Data collection was conducted in three stages, starting with cross-polarized photographs of the central teeth, which were analyzed using Adobe Photoshop and Camera RAW software to extract the L, a, b components for both opalescent and halo areas, followed by statistical analysis using SPSS. Results showed that 51% of participants were female and 49% male, with all exhibiting an opalescent area and 57% having a halo area.
Results: The opalescent area dimensions ranged from 0.20 to 0.83 mm, whereas the halo area ranged from 0.13 to 0.62 mm. Average values for L, a, and b in the opalescent zone were 68.94, 11.89, and 26.35, respectively, with mean ΔE values of 74.88 for the opalescent area and 77.52 for the halo zone. The opalescent zone was present in all participants, showing similar sizes across genders but slightly larger in men, whereas the halo zone was more common in women.
Conclusion: Men's teeth showed reddish and yellowish hues in the opalescent area, with no significant differences in the halo area, providing valuable insights for the design of aesthetic restorations and color coordination efforts.

Key Words: Central teeth, cross polarization, halo, opalescence, optical properties, photography

Received: 24-Sep-2025
Revised: 30-Nov-2025
Accepted: 10-May-2026
Published: 07-Sep-2026

Address for correspondence:
Dr. Mehrdad Kazemian, Department of Operative Dentistry, Dental School, Isf. C., Islamic Azad University, Isfahan, Iran.
E-mail: m.kazemian@khuisf.ac.ir

INTRODUCTION

In the realm of restorative dentistry, the esthetic integration of dental restorations with natural teeth is paramount. Despite the importance of opalescence in achieving this integration, many studies have downplayed its significance, often labeling it as the least critical factor in successful restoration.[1-3] However, we contend that opalescence is as vital as other features that contribute to the overall esthetic

Access this article online

Website: www.drj.ir
www.drjjournal.net
www.ncbi.nlm.nih.gov/pmc/journals/1480
DOI: 10.4103/drj.drj_554_25

How to cite this article: Raddanipour A, Kazemian M, Gholizadeh S. Study esthetic restoration of maxillary central teeth: Optical properties and color coordination in young adults in Isfahan. Dent Res J 2026;23:32.

quality of dental restorations. Tooth color matching remains one of the most empirically misunderstood aspects of dentistry, largely due to insufficient emphasis in dental education. The essence of restorative dentistry lies in esthetics, and improper color matching can lead to numerous failures in achieving a natural appearance.[4,5]

This study aims to delve into the optical properties of opalescence and the halo effect in the incisal area of central teeth among young individuals aged 20–30 in Isfahan. By extracting and analyzing laboratory information related to these properties, this research seeks to enhance the understanding of how opalescence influences tooth color and its practical application in the reconstruction of dental restorations by both dentists and dental laboratory technicians. To provide context for this investigation, we will outline the dimensions, limits, and relevant variables associated with the study of tooth color.[6-8] Color is inherently subjective, relying on three essential elements for its perception: light as a physical stimulus, the eye as the receiver, and individual perception as the interpreting agent. This means that color is not an intrinsic property of an object but rather a subjective experience shaped by individual significance.[9-12] Various systems and theories exist for classifying colors using precise methodologies. The Munsell color system serves as a foundational framework for classifying colored objects in three dimensions, akin to how a solid object is defined by its physical dimensions – length, width, and height.[13-17]

Color can be accurately defined by three main properties: hue, chroma, and value. Each property varies depending on the classification system employed. The Munsell system primarily offers a visual description, while the CIELAB color system provides a more quantitative analysis. The latter has been widely adopted in dentistry for quantitative color determination and remains a common method for visually describing color attributes.[15-18]

In restorative dentistry, a common issue arises when a restoration possesses a high value, making it excessively bright and easily recognizable, which detracts from the overall esthetic appeal, particularly in metal-ceramic prostheses.[19] Given the increasing patient demand for esthetic restorative treatments, the lack of proper simulation, and matching of opalescence in these procedures often leads to dissatisfaction among patients. There exists a significant gap in knowledge regarding the types of opalescence and an understanding of its spectral importance in aesthetic restorations, which is crucial for both dentists and dental prosthetic technicians. To address this gap, it is imperative to establish a scientific assessment criterion that identifies the types, distribution, and severity of opalescence and halo effects in the central teeth of individuals aged 20–30 years.[20-24] This assessment will help determine the prevalence of these properties and guide decisions regarding their simulation. The analysis will rely on color spectra obtained from the visual effects of tooth structure through standardized photography, taking into account factors such as lens distance, angle to the patient, and other environmental elements. In light of these considerations, the present study aims to investigate the prevalence of opalescence and halo effects in the central teeth of young adults in Isfahan using polarized photography.[25-28] By exploring these aspects, we hope to provide a clearer understanding of how these optical properties contribute to the overall aesthetics of dental restorations, ultimately leading to improved patient outcomes and satisfaction. The results of this study could serve as a valuable resource for dental professionals seeking to enhance their restorative practices and achieve more natural-looking results.

Research objectives

The primary objective of this study is to determine the prevalence and extent of opalescence and halo optical characteristics in the central teeth of young individuals aged 20–30 years in Isfahan, utilizing cross-polarized photography. To achieve this, several subobjectives will be addressed: first, to ascertain the Lab values of the incisal opalescence and halo zones; second, to evaluate the color ranges of both the incisal halo and opalescence zones; third, to measure the sizes of these zones; fourth, to identify the presence or absence of a halo; and finally, to analyze these features in relation to gender. The practical aim of this research is to apply the *Result*s on the prevalence of opalescence and halo in central teeth to enhance the reconstruction of incisal edges in composite and ceramic restorations. Key research questions guiding this investigation include inquiries into the Lab values of the incisal opalescent and halo zones, whether these values differ, the color ranges of both zones, their respective sizes, the presence of an incisal halo, and potential gender differences in these characteristics. By addressing these objectives and questions, the study seeks to provide valuable insights that can inform dental practices and improve aesthetic restoration techniques.

This article shows the structure and optical properties of teeth, along with relevant research, and outlines methods for measuring color and its historical context. Understanding how light interacts with teeth is essential for dentists aiming to create biomimetic restorations.[28] While the three main components of color – hue, value, and chroma – are often emphasized, an important factor frequently overlooked in cosmetic dentistry is the translucency of teeth.[29] Translucency refers to the extent to which light can pass through a surface or scatter within an opaque medium.[30,31] The incisal third of the tooth exhibits the highest translucency, primarily due to the thinner layer of dentin at the incisal edges. Among all teeth, the maxillary central incisors are particularly prominent and visible, serving as the foundation of an attractive smile.[32] Consequently, the aesthetic properties of these incisors are crucial in shaping the overall appearance of a smile.[33,34] Gaining a deeper understanding of how translucency and light interaction influence the aesthetics of maxillary central teeth is vital for achieving natural-looking and realistic dental restorations. The optical characteristics of these teeth, especially in the incisal area, can significantly aid dentists in crafting a beautiful, natural smile.

Optical properties of teeth

In physics, color is primarily known as light. The interaction between human teeth and light, as well as the interaction between restorative materials and light, has been investigated comparatively several times in studies (6). Tooth color is determined by a combination of its optical properties. When light strikes a tooth, four phenomena related to the interaction of the tooth with the light flux can be described (36): (1) transmission of light through the tooth, (2) specular reflection at the surface, (3) diffuse reflection at the surface, and (4) absorption and scattering of light by tooth tissues. Tooth color has been shown to result from volumetric scattering of light (37,38).

Investigation of the optical properties of teeth

Vaarkamp *et al*. conducted measurements of light transmission through enamel and dentinal tubules that are 0.85 mm thick.[35-39] Hydroxyapatite crystals in enamel play a significant role in light scattering, while dentin's light scattering is primarily attributed to its tubules.[40,41] In addition, a study by Ko *et al*. examined how the light scattering power of enamel changes with decreasing mineral content, showing that demineralization increased the scattering coefficient by approximately threefold.[40-42] Spitzer and Ton Bosch analyzed the reflection and transmission of light from thin sheets of bovine and human enamel across wavelengths from 220 to 700 nm using a spectrophotometer. They identified an absorption peak at 270 nm in all spectra, which lies outside the range of natural human visible light (380–780 nm).[43] An *in vitro* study revealed a strong correlation between the color of 28 teeth from various patients who had their enamel removed and that of intact teeth, confirming that dentin primarily determines tooth color, with enamel contributing only slightly through scattering in the blue range.[8] Zijp *et al*. noted that thin slabs of human enamel appear pale blue when viewed in daylight and pale yellow when viewed in transmission.[44] Several researchers have also investigated the luminescence properties, including fluorescence and phosphorescence, of enamel and dentin.[43,45,46] Dentin exhibits fluorescence excitation peaks at 300, 325, 380, and 410 nm, with corresponding emission maxima around 350, 400, 450, and 520 nm.[40] Enamel has excitation peaks at 285 and 330 nm, with emission maxima at 360 and 410 nm.[43] For bovine enamel powder, an emission maximum was recorded at 400 nm.[46] The combined fluorescence from both dentin and enamel has been reported to enhance the perceived whiteness or value of teeth.[47] However, Ten Bosch and Coops found that when measuring tooth color samples under different light sources, fluorescence did not significantly contribute to the color observed in everyday lighting conditions.[48-52]

Review of the literature

In 2023, Mishra *et al*. conducted a study to analyze the translucency characteristics of the upper central incisal third among the Indian population, focusing on different age and gender groups. They gathered primary data from intraoral images of 140 subjects across four age categories, using digital imaging and software analysis to identify translucency patterns. Their *Result*s led to the development of a three-tiered classification system that highlights the prevalence of various translucency types based on age and gender.[53-59] Similarly, Baratieri *et al*. investigated the impact of polarizing filters on color accuracy in images obtained from color tables using a digital DSLR camera, macro lens, and ring flash. They found that results from digital photography with polarizing filters were more aligned with those from a spectroradiometer for low-value color tables, whereas high-value tables performed better without the filter.[60] In another 2022 study, Baratieri *et al*. explored new trends in tooth color matching through various selection methods. Their results indicated that relying solely on digital images for color matching led to a decrease in ΔE, whereas using a spectrophotometer showed no advantage over visual color guide tabs. The study concluded that both digital photography and spectrophotometric measurements resulted in fewer color discrepancies compared to traditional methods using color tabs.[60]

MATERIALS AND METHODS

The study used a descriptive-analytic design and was conducted at the Islamic Azad University, Khorasgan Branch, in Isfahan, during April 1404. The statistical population consisted of young individuals aged 20–30 years residing in Isfahan. The study specifically focused on the central teeth of participants within this age group who did not have orthodontic appliances, fillings, cosmetic restorations, or specific dental abnormalities such as amelogenesis imperfecta or enamel defects. Eligible participants were included in the study after providing written consent. To determine the necessary sample size for estimating the average lab value in the population, the formula $n = ([z\_(\alpha/2) \times \sigma]/\varepsilon)^2$ was utilized, where ε represents accuracy and α denotes the error level. With a 5% error rate and an accuracy of 15% of the standard deviation (SD) ($\varepsilon = 0.15\ \sigma$), a sample size of 171 individuals was calculated. After accounting for a 10% increase, a total of 190 samples were selected for the study. The data collection tools included digital photography hardware equipment.

Figure 1 shows the core digital photography system used for standardized image capture. The Canon EOS 5D Mark III DSLR camera, paired with a dedicated macro lens and ring flash, was essential for obtaining high-resolution, consistent close-ups. This professional setup ensured all photographs had uniform magnification, lighting, and focus, forming the reliable foundation for all subsequent color and optical analysis in the study.

Figure 2 shows how to achieve true color data free from surface glare, polarizing filters were employed. A linear polarizing film was fitted over the ring flash, while a complementary circular polarizer was mounted on the camera lens. By crossing these filters, specular reflections were eliminated, allowing the camera to capture the tooth's subsurface light scattering and intrinsic color, which is critical for measuring opalescence and halo effects.

Figure 3 presents the standardization tools are displayed, including a cheek retractor for unobstructed vision and a crucial gray card. This card, placed adjacent to the tooth during photography, provided a known reference point ($L = 52$, $a = 0$, $b = 0$) for precise color calibration in software during postprocessing, ensuring that all measured L* a*b* values were accurate and consistent across every participant's photograph.

The study utilized specialized software for digital photo analysis and standardization, specifically Adobe Camera RAW 17.2 and Adobe Photoshop CC2023. A highly calibrated digital photography technique was employed to capture color information from the teeth, with a detailed methodology for using Photoshop to standardize images and extract this color data. The photographic setup included a Canon EOS 5D Mark

Figure 1: Digital SLR body: Canon EOS 5D Mark III, compatible macro lens: Canon macro lens EF 100 mm 1:2.8 USM, canon macro ring flash.

Figure 2: K and F liner polarizer film sheet, B + W polarizer filter NANO CPL-HAZE.

III digital camera, a macro lens, a ring flash, and polarized filters. Images were captured with accurate and continuous exposure in RAW format, utilizing a gray card positioned correctly for color analysis. The process involved several precise considerations: color images were recorded in RAW format, a white balance of 5600 Kelvin was applied, and manual exposure settings were used for optimal color accuracy. Figure 4 shows the camera's configuration menu is displayed, highlighting the critical settings for color fidelity. Images were captured in RAW format to retain maximum data, a custom white balance of 5600K was set for consistent color temperature, and exposure was manually controlled. This rigorous protocol guaranteed that the color information extracted was a true representation of the tooth's optical properties.

In the fourth case, the same magnification ratio was used for all the stained images of all the teeth of all the samples, and subsequently, the flash ring was placed at the same distance from the teeth. While setting the flash and camera in manual modes, the flash output was tested to find the right amount of flash power for the right exposure. Once the right settings were found, the exposure was always the same because the settings remained manual (the camera settings were the same, and the distance of the camera and flash from the teeth remained unchanged). In order to optimize the staining environment, the samples were photographed in a fixed location with the same lighting conditions. Furthermore, since most people's teeth are seen in a vertical position at a distance of 30 cm (25–35 cm), this was considered the optimal position for placing the patient for the shade assessment. As the patient's tooth shade analysis is performed in a vertical position, face to face with the dentist, at conversational distance. Another important aspect of controlling the shade analysis environment was that the teeth had to remain hydrated, as dry teeth become much brighter, which was also taken into account when photographing. Figure 5 shows the importance of maintaining tooth hydration during imaging. A dehydrated tooth appears overly bright and opaque, which can obscure the subtle optical phenomena being studied.

Ensuring teeth remained moist was a vital step to accurately capture the natural translucency and color dynamics of the opalescent and halo zones, preventing artificial data skew.

Accurate color photography protocol

When capturing the image, a 1 cm × 1 cm gray card was used for exposure calibration, which was later performed in Adobe Camera Raw, with values of $L = 52$, $a = 0$, and $b = 0$, measured in the CIELAB color model. The gray card was placed as close to the incisal edge of the tooth as possible, in a vertical position.

Figure 6 illustrates the precise placement of the 1 cm × 1 cm gray card during photography. Positioned vertically and as close as possible to the incisal edge of the central tooth, this card served as

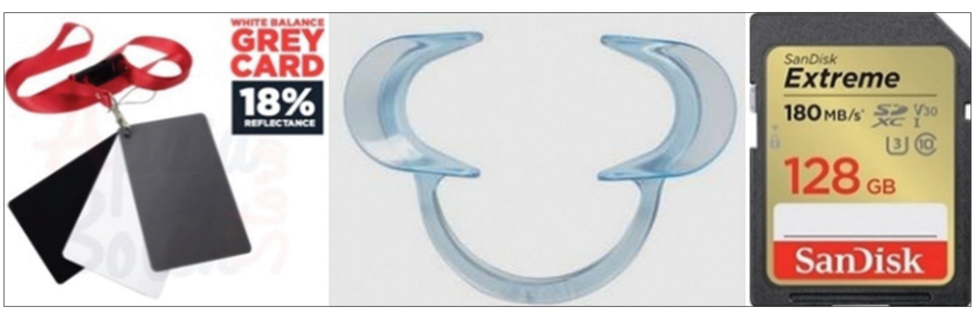

Figure 3: Gray card, cheek retractor, memory card.

Figure 4: RAW format selection, custom white balance setting, manual exposure adjustment option.

the absolute reference for color calibration. Its known neutral values (*L* = 52, *a* = 0, *b* = 0) allowed for software correction of any lighting inconsistencies, ensuring the tooth's measured L*a*b* values were scientifically accurate.

The shooting was done in Raw file format because it is uncompressed and has the most color information and can also be easily corrected if the camera settings were initially set incorrectly. The camera's manual settings were ISO200, F/7.1, shutter speed 1/251, flash on manual mode, and white balance on K and temperature 5600. The magnification was set to 1:1.5. This allowed the incisors and gray card to be evenly lit in the image. Figure 7 shows a test image captured with the finalized manual camera settings. The settings – ISO200, F/7.1, shutter speed 1/251, and a 5600K white balance – were rigorously determined and locked for all participants. This consistency ensured that every photograph was exposed identically, creating a uniform dataset where color differences truly reflected variations in tooth optics, not camera variables.

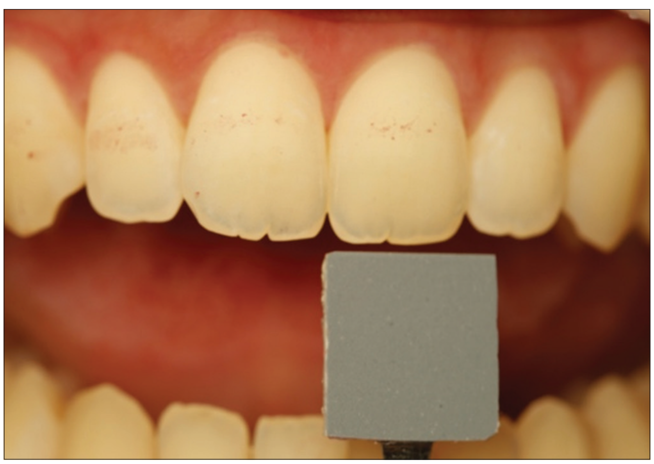

Figure 5: Dehydrated teeth when taking the photo.

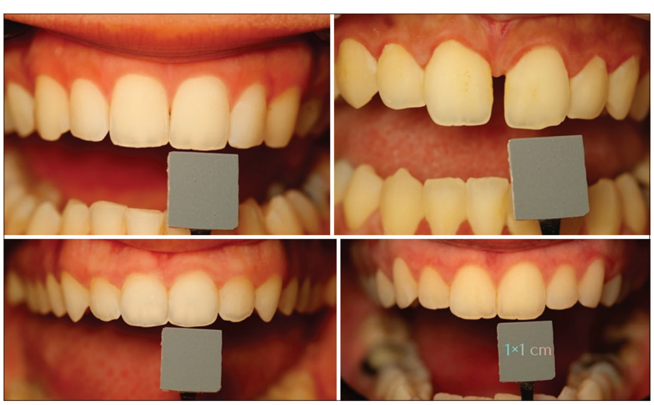

Figure 6: Size and position of the gray card.

A light polarizing sheet was cut to the shape of the flash surface and placed on the flash ring. A circular polarizing filter was also mounted on the macro lens so that it crossed with the polarizing sheet placed on the flash, which resulted in the elimination of reflected light from the tooth surfaces and reduced the brightness of the teeth by about 30%, which improved the visualization and evaluation of color.

Setting up Camera Raw Lab (set up) and color analysis in photoshop

Adobe Camera Raw is provided with Photoshop. This program is suitable for simple analysis that is done to extract color values from images. The procedure was as follows: First, the image was opened in Adobe Camera Raw. Figure 8 shows that the histogram is set to read color in red, green, blue (RGB) by default. The default histogram settings in Adobe Camera Raw are displayed, showing the color readout in the RGB color space. As this model is device-dependent and less ideal for scientific color measurement, this figure shows the initial state before conversion to the standardized CIELAB color space, which is used universally in dental color science for its perceptual uniformity.

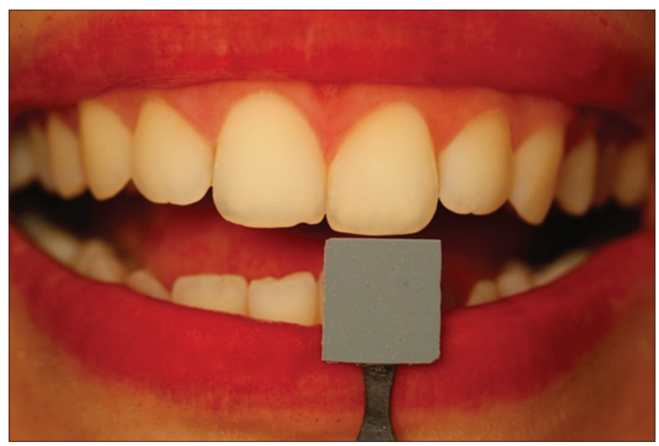

Figure 7: Test image with manual camera settings selected.

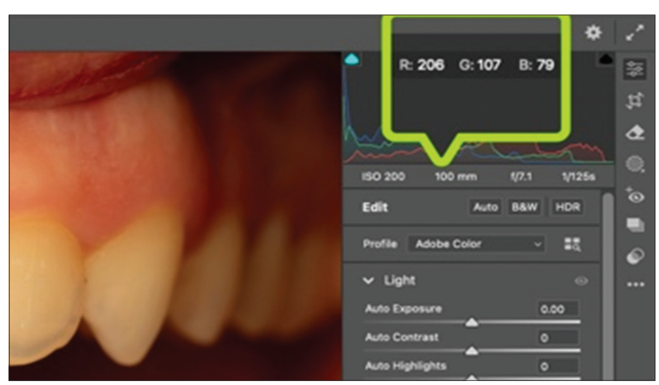

Figure 8: Default red, green, blue settings in photoshop.

We changed the settings to read Lab by hovering over the histogram and pressing the Control key and clicking at the same time. Figure 9 demonstrates the simple keyboard shortcut (Control + Click) used to convert the software's histogram readout from the RGB color space to the CIELAB (L*a*b*) system. This crucial step allowed the researchers to measure color in the same three-dimensional model used throughout the study, ensuring all collected data was directly comparable and met scientific standards.

Figure 9: How to convert the red, green, blue system to the Lab system.

Figure 10 shows that the process of image standardization using the gray card is depicted. The exposure slider in Adobe Camera Raw was adjusted until the cursor placed on the gray card registered an *L* = 52. This action neutralized any minor exposure shifts across different photo sessions, guaranteeing that all subsequent color measurements from the teeth were based on a perfectly calibrated baseline.

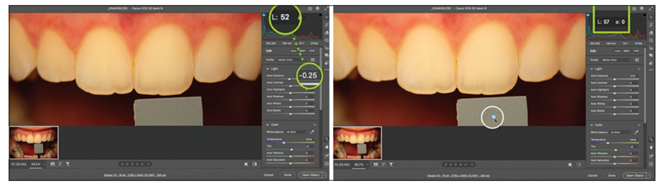

Figure 10: How to standardize an image using a gray card.

We placed the mouse on the gray card in the image closest to the tooth we wanted to examine and moved it in small circles. At the same time, we paid attention to the L value in the histogram. If the *L* value did not read 52, we moved the exposure slider left or right until that number was indicated.

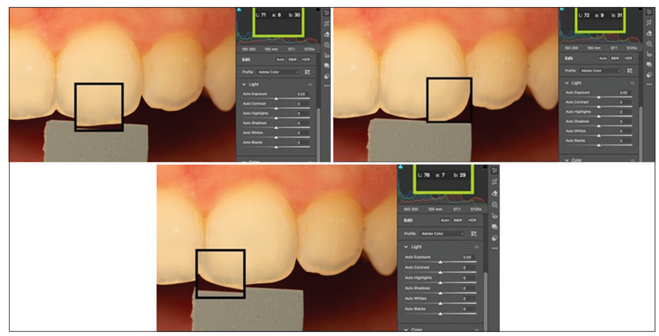

Figure 11: How to read Lab color values in opalescent and halo areas after the standardization stage.

Then, we opened the Info palette in Photoshop, clicked on the eyedropper, and activated the Lab color option. After that, to measure the L, a, and b indices, we divided the tooth into three parts: the mesial third, the middle third, and the distal third. For each part, in both the halo and opalescent areas, we recorded the lowest and highest L, a, b values by moving the mouse along the opalescent area and the halo area. Later, in the data analysis stage, the average of the highest and lowest values was calculated separately for each of the thirds. Figure 11 shows the final stage of data extraction within Adobe Photoshop. With the image standardized, the Info palette was set to read L*a*b* values. The cursor was then meticulously moved along the opalescent and halo areas in the mesial, middle, and distal thirds to record the highest and lowest L, a, and b values, providing the raw data for all statistical analyses.

The Ruler tool in Photoshop was used to determine the size of the opalescent area and halo (if any), and the largest size of the opalescent area and halo across the entire width of the tooth was measured and recorded. The color range of the opalescent area and halo was also determined by calculating the total L, a, b in a tooth, which is actually the average of the lowest and highest values for L, a, b across the entire tooth.

Data analysis method

Data analysis was performed at two levels: descriptive and inferential. At the descriptive level, for quantitative variables, indicators such as mean, SD, minimum, maximum, and 95% confidence interval were calculated and reported for the means, and for qualitative variables, frequency and percentage were presented. At the inferential level, appropriate statistical tests were used depending on the type of variable and data structure. To examine the difference in the mean of color components (L, a, b, and ΔE) in different areas of the opalescence and incisal halo, analysis of variance (ANOVA) with repeated measures was used. In cases where a significant difference was observed, Bonferroni-adjusted pairwise comparisons were used. An independent *t*-test was used to compare the means of quantitative variables between the two sexes (male and female). Furthermore, to analyze the relationship between qualitative variables, such as the presence or absence of the Halo area with gender, the Chi-square test was used. Data analysis was performed using IBM Corp. (2020). IBM SPSS Statistics for Windows (Version 27.0), Armonk, NY: IBM Corp, and in all statistical tests, a significance level of 0.05 ($\alpha = 0.05$) was considered.

RESULTS

In this article, the results of examining the optical properties of opalescence and Halo in maxillary central teeth in the young population of Isfahan city, using the polarized photography method, are presented. Data analysis was performed with the aim of answering the research questions, evaluating the research hypotheses, and examining the distribution and pattern of optical components in the studied samples. The studied properties included the color components L, a, b, the size of the opalescence and Halo areas, the prevalence of Halo, and the range of color changes (ΔE). First, a description of demographic characteristics and baseline optical indices was provided, and then color values were analyzed separately for distal, middle, and mesial regions for each of the two opalescent and halo regions. In addition to calculating the mean, SD, and 95% confidence interval for quantitative variables, statistical comparisons were also performed based on gender to allow for the examination of statistical differences between male and female groups in optical components.

Descriptive study of demographic characteristics and optical indices of samples

Among the 191 samples analyzed, 98 (51.3%) were female, and 93 (48.7%) were male. The results indicated that the halo region was present in 109 samples (57.1%), whereas 82 samples (42.9%) did not exhibit a halo. When examining the dimensions of the optical areas, the size of the opalescent zone across all samples ranged from 0.20 to 0.83 mm, with an average size of 0.545 mm and a SD of 0.12 mm. In the 109 samples that included a halo area, its size varied from 0.13 to 0.62 mm, with a mean size of 0.379 mm and a SD of 0.09 mm.

Results related to the LAB of the incisal opacities

The analysis of the samples revealed that out of 191 participants, 98 (51.3%) were female and 93 (48.7%) were male. The halo region was present in 109 samples (57.1%), whereas 82 samples (42.9%) showed no halo. The dimensions of the optical areas indicated that the opalescent zone ranged from 0.20 to 0.83 mm, with an average size of 0.545 mm and a SD of 0.12 mm. Among the samples with a halo, the size varied from 0.13 to 0.62 mm, averaging 0.379 mm with a SD of 0.09 mm. Descriptive statistics further detailed the L, a, and b values across the distal, middle, and mesial opacities. The average brightness (L) in the distal area was 41.66 (SD = 3.82), whereas in the middle and mesial areas, it was 23.71 (SD = 3.10) and 90.71 (SD = 3.85), respectively. The overall mean for L was 68.94 ± 3.23. For component a, measuring the green-red spectrum, the distal region averaged 12.66 (SD = 2.51), the middle region 10.93 (SD = 2.18), and the results region 10.84 (SD = 2.32), with an overall mean of 11.89 ± 2.13. In the blue-yellow spectrum (component b), the distal region averaged 26.33 (SD = 3.47), the middle region 27.38 (SD = 3.84), and the mesial region 26.14 (SD = 3.77), resulting in an overall mean of 26.35 ± 3.36. These results show significant variations in optical properties across different regions of the teeth, providing insights into the complexities of dental esthetics and the role of optical dimensions in determining color characteristics. Table 1 shows the descriptive statistics for the L, a, and b* color coordinates and ΔE (color difference) measured in the distal, middle, and mesial regions of the incisal opalescent zone. The data clearly illustrate the significant spatial variations in brightness, hue, and chroma across the tooth's incisal edge.

In the analysis of color difference (ΔE), the mean value for the distal region was found to be 72.71, with a SD of 3.05, resulting in a 95% confidence interval ranging from 72.28 to 73.15. For the middle region, the mean ΔE was 23.77, accompanied by a SD of 2.86 and a confidence interval of 76.82–77.64. In the mesial region, the mean ΔE value was 41.77, with a SD of 3.33 and a confidence interval of 76.94–77.89. Overall, the mean ΔE across all regions was calculated to be 88.74, with a SD of 2.67 and a confidence interval between 74.50 and 75.26. These results indicate significant variations in color differences across the different regions analyzed, emphasizing the complexity of dental esthetics.

The three-dimensional graphs presented in Figure 12 illustrate the distribution of color component values – brightness (L), green–red spectrum (a), and blue–yellow spectrum (b) – across the three incisal opacities. Notably, the variation in the density and positioning of points within the color space among

Table 1: Average LAB values in different areas of the incisal alveolar ridge

Variable	Range	Number	Minimum	Maximum	Mean±SD	95%CI	
						Lower Bound	Upper Bound
L	Distal	191	54.50	75.50	66.41±3.82	65.86	66.95
	Middle	191	61.00	78.00	71.23±3.10	70.79	71.68
	Mesial	191	58.50	81.50	71.90±3.85	71.35	72.44
	Total	191	59.50	75.50	68.94±3.23	68.48	69.40
A	Distal	191	6.00	21.50	12.66±2.51	12.30	13.02
	Middle	191	6.50	19.00	10.93±2.18	10.62	11.24
	Mesial	191	6.00	18.00	10.84±2.32	10.51	11.17
	Total	191	6.50	18.00	11.89±2.13	11.59	12.19
B	Distal	191	18.00	36.50	26.33±3.47	25.84	26.83
	Middle	191	16.50	37.50	27.38±3.84	26.83	27.93
	Mesial	191	16.50	37.50	26.14±3.77	25.60	26.68
	Total	191	17.50	35.50	26.35±3.36	25.87	26.82
ΔE	Distal	191	64.22	79.46	72.71±3.05	72.28	73.15
	Middle	191	69.70	83.20	77.23±2.86	76.82	77.64
	Mesial	191	67.27	85.03	77.41±3.33	76.94	77.89
	Total	191	67.99	80.54	74.88±2.67	74.50	75.26

Lightness (from black to white)=L. a=Green–Red axis=A. b=Blue–Yellow axis=B. Color difference (Delta E)=ΔE. SD: Standard deviation

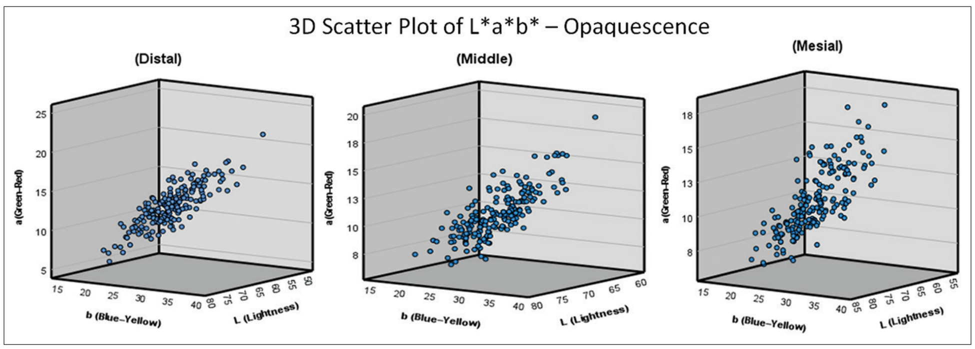

Figure 12: Three-dimensional scatter diagram of the L*a*b* color space in different areas of the central incisal alveolar ridge (Distal, Middle, Mesial).

the different areas is clearly observable, revealing distinct color patterns for each region. For the L component (brightness), values in the distal area ranged from 54.50–50.75, while the middle and mesial regions exhibited ranges of 0.61–8.78 and 5.58–5.81, respectively. The concentration of points in the middle and mesial areas is higher on the L axis, indicating greater brightness and light density in these regions compared to the distal area. The distal region also showed the largest variation in the a component, with values ranging from 0.6 to 21.50, whereas the middle and mesial regions had narrower ranges of 6.5–0.19 and 0.6–0.18, respectively, suggesting a broader variation in red hues in the distal region compared to the orange tones present. Regarding the b component (blue-yellow), values also varied among the regions: the distal region ranged from 0.18 to 5.36, while the middle and mesial regions had similar ranges of 16.5–5.37 and 16.50–37.50, respectively. These results point to a relatively consistent yet widespread presence of yellow color across the different areas of orange.

The symbol "< or >" indicates a statistically significant difference between regions ($P < 0.05$), and "=" indicates no significant difference. Table 2 shows the results of comparing the mean values of the four color components – L, a, b, and ΔE – across the distal, middle, and mesial incisal orange regions of the central teeth. A repeated-measures ANOVA revealed statistically significant differences among the regions for all variables ($P < 0.001$). According to the *post hoc* tests with Bonferroni correction, the differences in means for each color component were as follows: For component L (brightness), the mean value in the mesial region was significantly higher than in the middle region ($P = 0.001$), and the middle region, in turn, was significantly higher than the distal region ($P < 0.001$). In terms of component a (green-red), the mean value in the distal region was notably higher than in both the middle and mesial regions ($P < 0.001$), although there was no significant difference between the middle and mesial regions ($P = 0.001$). For component b (blue-yellow), the middle region's mean value exceeded those of the distal and mesial regions ($P < 0.001$), whereas the difference between the distal and mesial regions was not statistically significant ($P = 0.001$). Regarding the ΔE value (color difference), the mean ΔE in the middle and mesial regions was significantly greater than in the distal region ($P < 0.001$), but there was no significant difference between the middle and mesial regions ($P = 0.990$). Figures 12-15 illustrate the mean values of the color components, including L, a, b, and ΔE, categorized by distal, middle, mesial, and total incisal orange, along with their 95% confidence intervals. Figure 13 shows bar chart compares the mean L* value (lightness) across the three regions of the incisal opalescence. The results clearly show a statistically significant increase in brightness from the distal to the mesial region. This gradient in lightness is a critical optical characteristic that contributes to the vitality and depth of a natural tooth and must be considered when layering composite resins or ceramics.

Table 2: Mean, standard deviation, and repeated-measures analysis of variance results for color components in incisal orange areas

Variable	Area	Mean±SD	Statistic	*P*	Result
L	Distal	66.41±3.82	353.035	<0.001	Mesial > Middle > Distal
	Middle	71.23±3.10			
	Mesial	71.90±3.85			
A	Distal	12.66±2.51	129.537	<0.001	Distal > Middle=Mesial
	Middle	10.93±2.18			
	Mesial	10.84±2.32			
B	Distal	26.33±3.47	24.953	<0.001	Middle > Distal=Mesial
	Middle	27.38±3.84			
	Mesial	26.14±3.77			
ΔE	Distal	72.71±3.05	339.298	<0.001	Distal > Middle=Mesial
	Middle	77.23±2.86			
	Mesial	77.41±3.33			

Statistical comparisons between regions were performed using repeated measures ANOVA. The results of the post hoc tests (Bonferroni-adjusted) are reported in the "Result" column. ANOVA: Analysis of variance; SD: Standard deviation

Figure 14 shows the mean a* values, which represent the green–red axis of color. The distal region demonstrated a significantly higher a* value (more red) compared to the middle and mesial regions, which were statistically similar. Understanding this specific distribution of red hues within the opalescent zone is essential for achieving color harmony and avoiding restorations that appear monochromatic or artificially flat.

Figure 15 shows the mean b* values, indicating the blue-yellow spectrum. The data reveal that the middle region of the opalescent zone had a significantly higher b* value (more yellow) than both the distal and mesial regions. This pattern highlights another layer of complexity in natural tooth color, where a central concentration of yellow contributes to the overall warm undertone of the incisal edge.

Figure 16 illustrates the mean color difference (ΔE) values across the distal, middle, and mesial regions of the incisal opalescence. The results show a significantly lower ΔE in the distal region compared to the middle and mesial regions, which were statistically similar. This quantifies the distinct visual character of each zone and underscores that a single color of restorative material cannot accurately mimic the complex optical landscape of the natural incisal edge.

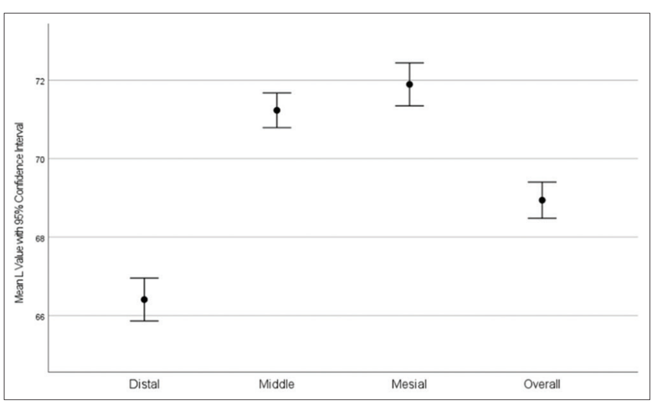

Figure 13: Mean L component (luminance) in different areas of incisal opacities with 95% confidence interval.

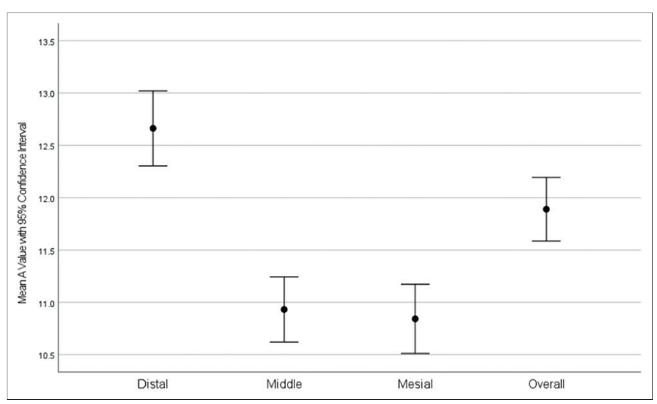

Figure 14: Mean A component (green–red) in different incisal opalescence areas with 95% confidence interval.

Results related to the LAB of the incisal halo area

In Table 3, descriptive statistics indicators including minimum, maximum, mean, SD, and 95% confidence interval for the values of L, a, b, and ΔE are presented separately for the distal, middle, and mesial areas of the incisal halo.

The analysis of the L component (luminance) showed that in the distal region, the mean luminance was 21.68, with a SD of 4.39 and a 95% confidence interval ranging from 38.67 to 04.69. In the middle region, the mean L value was higher at 45.72, with a SD of 4.56 and a confidence interval of 58.71–31.73. The mesial region showed a mean luminance of 06.73, accompanied by a SD of 4.68 and a confidence interval of 17.72–95.73. The mean L value across all regions was calculated to be 13.70 ± 4.68, with a confidence interval of 36.69–92.70.

DISSCUSION

For the a component (green–red spectrum), the distal region had a mean value of 14.08 (SD = 2.19), with a confidence interval between 13.66 and 14.49. In the middle region, the mean was 11.92 (SD = 2.08) with a confidence interval of 11.53–12.32, while the mesial region had a mean of 12.30 (SD = 2.35) and a confidence interval of 11.86–12.75. The overall mean for the a component across the three regions was 13.38 ± 1.96, with a confidence interval of 13.00–13.75. Regarding the b component (blue–yellow spectrum), the distal region's mean was 20.30 (SD = 2.68), with a confidence interval between 29.69 and 30.71. The middle region's mean was 30.22 (SD = 2.98), with a confidence interval of 29.65–30.79, while the mesial region recorded a mean of 29.68 (SD = 3.24) and a

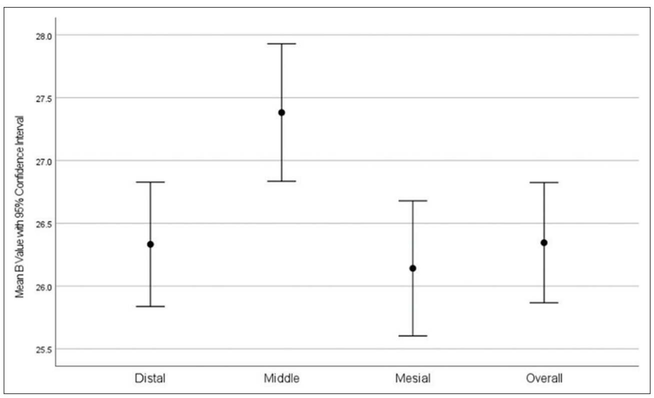

Figure 15: Mean B component (blue-yellow) in different areas of incisal opacities with 95% confidence interval.

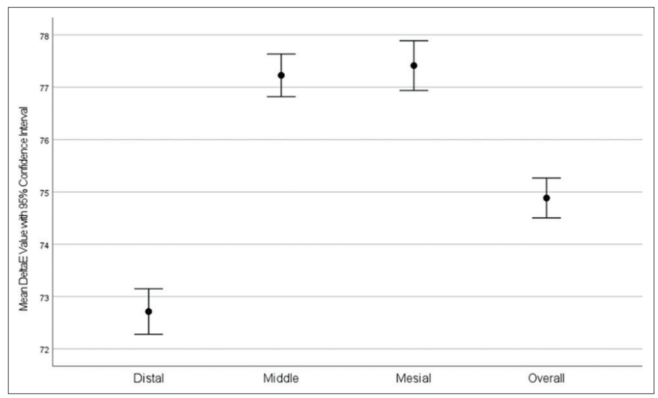

Figure 16: Mean ΔE (color difference) in different areas of incisal opacities with 95% confidence intervals.

Table 3: Average LAB values in different incisal halo areas

Variable	Area	Number	Minimum	Maximum	Mean±SD	95% CI	
						Lower bound	Upper bound
L	Distal	109	37.00	74.50	68.21±4.39	67.38	69.04
	Middle	109	38.00	78.50	72.45±4.56	71.58	73.31
	Mesial	109	39.50	79.00	73.06±4.68	72.17	73.95
	Total	109	38.50	76.00	70.13±4.14	69.35	70.92
A	Distal	109	7.50	18.50	14.08±2.19	13.66	14.49
	Middle	109	7.00	17.50	11.92±2.08	11.53	12.32
	Mesial	109	8.00	18.50	12.30±2.35	11.86	12.75
	Total	109	8.00	18.00	13.38±1.96	13.00	13.75
B	Distal	109	23.50	38.00	30.20±2.68	29.69	30.71
	Middle	109	22.00	38.50	30.22±2.98	29.65	30.79
	Mesial	109	22.00	37.00	29.68±3.24	29.07	30.30
	Total	109	23.00	35.50	29.93±2.65	29.42	30.43
ΔE	Distal	109	50.88	81.81	76.04±3.48	75.38	76.70
	Middle	109	50.46	85.18	79.52±3.85	78.79	80.25
	Mesial	109	53.16	85.37	79.96±3.73	79.25	80.67
	Total	109	52.47	82.26	77.52±3.29	76.90	78.15

Lightness (from black to white)=L. a=Green–Red axis=A. b=Blue–Yellow axis=B. Color difference (Delta E)=ΔE. SD: Standard deviation confidence interval of 29.07–30.30. The overall mean for the b component was estimated at 29.93 ± 1.65, with a confidence interval of 29.42–30.73. Finally, the mean color difference (ΔE) in the distal region was 76.04 (SD = 3.48), with a confidence interval of 75.38–70.76. In the middle region, the mean ΔE was 79.52 (SD = 3.85), with a confidence interval of 78.79–80.25, while the mesial region showed a mean of 79.96 (SD = 73.3) and a confidence interval of 79.25–80.67. The overall mean ΔE across all regions was 77.52 ± 3.29, with a confidence interval of 76.90–78.15 between them. Although in the study of Siddharth Mishra who classified the translucency patterns, as well as in the study of Mohammed Alshehri who classified the types of opalescence, and in the study of Sillas Duarte who provided a classification for opalescence, all tried to improve the reconstruction of the opalescent area of natural teeth with restorative materials, determining the opalescent patterns alone and without examining the L, a, b parameters in different parts of the opalescent area and the halo of the tooth does not lead to a reconstruction that is consistent with the natural tooth. Therefore, to complete and continue this research and the lack of such a study in the research history, the necessity of conducting the present study became apparent. Foundational studies by Kamishima *et al*. and Yu and Lee crucially investigate the properties of resin composites,[49,50] while clinical guides like Baratieri *et al*. outline restorative principles;[52] however, these focus on synthetic materials and techniques rather than providing quantitative baselines for natural tooth structure. Research on natural teeth, such as the early work by Brodbelt *et al*. on enamel translucency[53] and the highly relevant recent study by Mishra *et al*. classifying translucency in an Indian population,[56-59] offer a more direct comparison. However, differentiates itself by moving beyond pattern classification or general translucency to provide a deeper, quantitative deconstruction of specific incisal optical zones (opalescence and halo) using cross-polarized photography and precise CIELAB coordinates. While broader context on shade matching and age-related changes is covered by authors like Fondriest and Ketterl,[51,57] and modern digital analysis is echoed in work by Xia and Xiong,[56] which in this study uniquely fills a gap by delivering a detailed, quantitative map of the L*a*b* values and dimensions of these zones in a young Iranian population, thus offering a direct scientific basis for biomimetic restoration that prior studies often only addressed conceptually.

Rajaei *et al*.,[61] who focus on creating the advanced biomaterials that can replicate this beauty while enduring the mouth's harsh environment. Their research journey begins with strengthening the very foundations of restorative care, such as reinforcing crown ceramics with nanoparticles[61,62] and improving filling cements[63] for greater durability, and extends into ensuring these materials biologically harmonize with the body through bioactive compounds that encourage bone integration.[62,64-67] This pursuit of synergy has evolved into pioneering the future of dental care, where 3D bioprinting crafts scaffolds for tissue regeneration,[68-72] custom-fit structures are built with digital precision,[68] and the performance of new materials is predicted using computer simulations and artificial intelligence[69,73-76] while in this study, we provide the critical "map" of natural tooth aesthetics, their work builds the "vehicle" – delivering a new generation of restorations that are not only visually indistinguishable from nature but are also engineered for superior strength, integration, and long-term clinical success.

CONCLUSION

The opalescent zone is a consistent and significant optical feature present in all individuals, with sizes being approximately equal between men and women. The halo zone, however, appears in about half of the individuals and is more prevalent in women, where it is slightly larger and brighter. In the opalescent zone of men's teeth, there is a greater tendency toward redness and yellowness, although no significant differences were observed in the halo zone. Women's teeth tend to have a slightly higher brightness in the opalescent zone. While gender differences in overall color perception (ΔE) were not significant, notable differences were found in the basic color components (b*, a*, and L*). These results have practical implications for the design of aesthetic restorations, including veneers and laminates, as well as for color coordination in dental treatments. Future studies could investigate the effects of age, tooth background color, and environmental factors on opalescence and halo, examine CIELAB values in lateral, canine, and posterior teeth, combine colorimetric analysis with enamel texture studies using SEM or polarized microscopy, and develop a tooth color database reflective of the native Iranian population for use in smile design and digital treatments. However, this study does have limitations, including the lack of similar detailed research focused on the b*, a*, and L* values in opalescence and halo, the dependence of data on light quality and photography despite control measures through cross-polarized techniques, and the exclusive focus on maxillary central teeth within a specific age group.

Acknowledgment

The authors would like to express their sincere gratitude to the Department of Operative Dentistry, Dental School, Isf. C., Islamic Azad University, Isfahan, Iran, for providing the necessary resources and facilities to conduct this research.

Financial support and sponsorship

Nil.

Conflicts of interest

The authors of this manuscript declare that they have no conflicts of interest, real or perceived, financial or non-financial in this article.

REFERENCES

1. Leven A. Layers: An atlas of composite resin stratification. British Dental Journal 2013;214:319. https://doi.org/10.1038/sj.bdj.2013.317.
2. Gopikrishna V. Sturdevant's Art and Science of Operative Dentistry-E Book: Second South Asia Edition. Elsevier Health Sciences; 2018.
3. Yamamato M. Metal-Ceramics: Principles and Methods of Makoto Yamamato. Chicago: Quintessence Publishing Co Inc.; 1985. p. 268-90.
4. Chu SJ. The science of color and shade selection in aesthetic dentistry. Dent Today 2002;21:86-9.
5. Villarroel M, Fahl N, De Sousa AM, De Oliveira OB Jr. Direct esthetic restorations based on translucency and opacity of composite resins. J Esthet Restor Dent 2011;23:73-87.
6. Vanini L. Light and color in anterior composite restorations. Pract Periodontics Aesthet Dent 1996;8:673-82.
7. Ardu S, Feilzer AJ, Devigus A, Krejci I. Quantitative clinical evaluation of esthetic properties of incisors. Dent Mater 2008;24:333-40.
8. ten Bosch JJ, Coops JC. Tooth color and reflectance as related to light scattering and enamel hardness. J Dent Res 1995;74:374-80.
9. Devoto W, Saracinelli M, Manauta J. Composite in everyday practice: How to choose the right material and simplify application techniques in the anterior teeth. Eur J Esthet Dent 2010;5:102-24.
10. Komine F, Blatz MB, Yamamoto S, Matsumura H. A modified layering technique to enhance fluorescence in glass-infiltrated aluminum oxide ceramic restorations: Case report. Quintessence Int 2008;39:11-6.
11. Monteiro P, Brito P, Pereira J, Alves R. The importance of the optical properties in dental silica-based ceramics. J Calif Dent Assoc 2012;40:476-81.
12. Cho MS, Yu B, Lee YK. Opalescence of all-ceramic core and veneer materials. Dent Mater 2009;25:695-702.
13. Abulhamael AM, Tandon R, Alzamzami ZT, Alsofi L, Roges RA, Rotstein I. Treatment decision-making of cracked teeth: Survey of American endodontists. J Contemp Dent Pract 2019;20:543-7.
14. Olivieri JG, Elmsmari F, Miró Q, Ruiz XF, Krell KV, García-Font M, *et al*. Outcome and survival of endodontically treated cracked posterior permanent teeth: A systematic review and meta-analysis. J Endod 2020;46:455-63.
15. Magne P. IDS: Immediate dentin sealing (IDS) for tooth preparations. J Adhes Dent 2014;16:594.
16. Senawongse P, Srihanon A, Muangmingsuk A, Harnirattisai C. Effect of dentine smear layer on the performance of self-etching adhesive systems: A micro-tensile bond strength study. J Biomed Mater Res B Appl Biomater 2010;94:212-21.
17. Ghiggi PC, Steiger AK, Marcondes ML, Mota EG, Burnett LH Júnior, Spohr AM. Does immediate dentin sealing influence the polymerization of impression materials? Eur J Dent 2014;8:366-72.
18. Magne P, Belser U. Biomimetic Restorative Dentistry. 2nd ed. Pascal Magne / Urs C. Belser/quintessence-publishing; 2022.
19. Azita MT, Kaveh S, Mehran N, Arash Z, Translators. Modern Principles in Fixed Dental Prostheses. 1st ed., Vol 2. Tehran: Shayan Daraham; 2016.
20. Maryam RD, Zahra Q, Nika M, Translators. Basics of Color in Dentistry: Color Selection and Matching in Cosmetic Dentistry. 1st ed. Tehran: Shayan Daraham; 2010.
21. Hassan A, Yalda D. Aesthetics in Dental Prostheses. 2nd ed. Tehran: Royan Pajouh; 2017.
22. Mehdi M, Javad JK, Sajjad PH, Yousef P, Elham R. Photography in Dentistry. Supervised By: Vahid Karimi. Tehran: Shayan Daraham; 2016.
23. Elham R, Mehdi M, Yousef P, Javad JK, Sajjad PH, Translators. Photography in Dentistry: Theoretical and Practical Principles in Modern File Making. Under the Supervision of: Vahid Karimi. 1st ed. Tehran: Shayan Daraham; 2016.
24. Nader KR. Digital Photography Guide. 4th ed. Tehran: Science Publishing Center; 2014.
25. Sampaio CS, Atria PJ, Hirata R, Jorquera G. Variability of color matching with different digital photography techniques and a gray reference card. J Prosthet Dent 2019;121:333-9.
26. Zhang LW, Bi AL, Li Q, Bi HS. Application of fiber photometry in neuroscience research. Sheng Li Xue Bao 2021;73:306-14.
27. Rashid F, Jamayet NB, Farook TH, Al-Rawas M, Barman A, Johari Y, *et al*. Color variations during digital imaging of facial prostheses subjected to unfiltered ambient light and image calibration techniques within dental clinics: An *in vitro* analysis. PLoS One 2022;17:e0273029.
28. Sikri VK. Color: Implications in dentistry. J Conserv Dent 2010;13:249-55.
29. Joiner A. Tooth colour: A review of the literature. J Dent 2004;32 Suppl 1:3-12.
30. Hasegawa A, Ikeda I, Kawaguchi S. Color and translucency of *in vivo* natural central incisors. J Prosthet Dent 2000;83:418-23.
31. Lee, Yong-Keun. "Translucency of human teeth and dental restorative materials and its clinical relevance." Journal of Biomedical Optics 2015;20:045002-045002.

32. Alsulaimani FF, Batwa W. Incisors' proportions in smile esthetics. J Orthod Sci 2013;2:109-12.
33. da Cunha LF, Gonzaga CC, Saab R, Mushashe AM, Correr GM. Rehabilitation of the dominance of maxillary central incisors with refractory porcelain veneers requiring minimal tooth preparation. Quintessence Int 2015;46:837-41.
34. Bhuvaneswaran M. Principles of smile design. J Conserv Dent 2010;13:225-32.
35. Bayindir F, Gozalo-Diaz D, Kim-Pusateri S, Wee AG. Incisal translucency of vital natural unrestored teeth: A clinical study. J Esthet Restor Dent 2012;24:335-43.
36. Jahangiri L, Reinhardt SB, Mehra RV, Matheson PB. Relationship between tooth shade value and skin color: An observational study. J Prosthet Dent 2002;87:149-52.
37. van der Burgt TP, ten Bosch JJ, Borsboom PC, Kortsmit WJ. A comparison of new and conventional methods for quantification of tooth color. J Prosthet Dent 1990;63:155-62.
38. O'Brien WJ, Johnston WM, Fanian, F. Double-layer color effects in porcelain systems. Journal of Dental Research 1985;64:940-3.
39. Vaarkamp J, ten Bosch JJ, Verdonschot EH. Propagation of light through human dental enamel and dentine. Caries Res 1995;29:8-13.
40. Ten Bosch JJ, Zijp JR. Optical properties of dentin. In: Thylstrup A, Leach SA, Qvist V, editors. Dentine and Dentine Reactions in the Oral Cavity. Oxford, England: IRL Press; 1987. p. 59-65.
41. Zijp JR, Bosch JJ. Theoretical model for the scattering of light by dentin and comparison with measurements. Appl Opt 1993;32:411-5.
42. Ko CC, Tantbirojn D, Wang T, Douglas WH. Optical scattering power for characterization of mineral loss. J Dent Res 2000;79:1584-9.
43. Spitzer D, Ten Bosch JJ. The absorption and scattering of light in bovine and human enamel. Calcif Tissue Res 1975;17:129-37.
44. Zijp JR, ten Bosch JJ, Groenhuis RA. HeNe-laser light scattering by human dental enamel. J Dent Res 1995;74:1891-8.
45. Hefferren JJ, Hall JB, Bennett E. Luminescence as a tool to study enamel interactions. In: Fearnhead RW, Stack MV, editors. Tooth Enamel II. Bristol: John Wright; 1971. p. 161-5.
46. Booij M, ten Bosch JJ. A fluorescent compound in bovine dental enamel matrix compared with synthetic dityrosine. Arch Oral Biol 1982;27:417-21.
47. Terry DA, Geller W, Tric O, Anderson MJ, Tourville M, Kobashigawa A. Anatomical form defines color: Function, form, and aesthetics. Pract Proced Aesthet Dent 2002;14:59-67.
48. Schmeling M, DE Andrada MA, Maia HP, de Araújo EM. Translucency of value resin composites used to replace enamel in stratified composite restoration techniques. J Esthet Restor Dent 2012;24:53-8.
49. Kamishima N, Ikeda T, Sano H. Color and translucency of resin composites for layering techniques. Dent Mater J 2005;24:428-32.
50. Yu B, Lee YK. Influence of color parameters of resin composites on their translucency. Dent Mater 2008;24:1236-42.
51. Fondriest J. Shade matching in restorative dentistry: The science and strategies. Int J Periodontics Restorative Dent 2003;23:467-79.
52. Baratieri LN, Araújo EM, Monteiro JR. Composite Restorations in Anterior Teeth. Fundamentals and Possibilities. New York: Quintessence; 2005.
53. Brodbelt RHW, O'brien WJ, Fan PL, Frazer-Dib JG, Yu R. Translucency of human dental enamel. Journal of dental research, 1981;60:1749-53.
54. Lee YK, Lim BS, KIM CW. Difference in colour and colour change in dental resin composites by the background. J Oral Rehabil 2005;32:227-33.
55. Yamato M. Metal Ceramics: Principles and Methods of Makato Yamato. Chicago (IL): Quint Publishing Co. Inc.; 1985. p. 345-58.
56. Xia H, Xiong F. Clinical threshold of the translucency parameter of maxillary central incisors. Dent Mater J 2021;40:547-51.
57. Ketterl W. Age-induced changes in the teeth and their attachment apparatus. Int Dent J 1983;33:262-71.
58. Nadig RR, Usha G, Kumar V, Rao R, Bugalia A. Geriatric restorative care – The need, the demand and the challenges. J Conserv Dent 2011;14:208-14.
59. Mishra S, Murthy P, Ahuja D, Thomas MS, Natarajan S, Pai U. Translucency characteristics of permanent maxillary central incisor in Indian population: An analytical cross-sectional study. J Conserv Dent Endod 2023;26:651-6.
60. Baratieri LN, Monteiro Jr S, de Melo TS, Ferreira KB, Hilgert LA, Schlichting LH, Bernardon JK, et al. Preparation and Restoration of Class IV with Composite Resin. In: Restorative Dentistry - Fundamentals and Techniques. 1st ed. São Paulo: Santos; 2010. p. 203-39.
61. Rajaei A, Kazemian M, Khandan A. Investigation of mechanical stability of lithium disilicate ceramic reinforced with titanium nanoparticles. Nanomed Res J 2022;7:350-9.
62. Khandan A, Abdellahi M, Ozada N, Ghayour H. Study of the bioactivity, wettability and hardness behaviour of the bovine hydroxyapatite-diopside bio-nanocomposite coating. J Taiwan Inst Chem Eng 2016;60:538-46.
63. Azimi R, Shahgholi M, Khandan A. Fabrication and characterization of reinforced glass ionomer cement by zinc oxide and hydroxyapatite nanoparticles. Heliyon 2024;10:e39063.
64. Khandan A, Abdellahi M, Barenji RV, Ozada N, Karamian E. Introducing natural hydroxyapatite-diopside (NHA-Di) nano-bioceramic coating. Ceram Int 2015;41:12355-63.
65. Khandan A, Karamian E, Bonakdarchian M. Mechanochemical synthesis evaluation of nanocrystalline bone-derived bioceramic powder using for bone tissue engineering. Dent Hypotheses 2014;5:155-61.
66. Khandan A, Nassireslami E, Saber-Samandari S, Arabi N. Fabrication and characterization of porous bioceramic-magnetite biocomposite for maxillofacial fractures application. Dent Hypotheses 2020;11:74-85.
67. Khademi A, Khandan A, Iranmanesh P, Heydari M. Development of a 3D bioprinted alginate-gelatin hydrogel scaffold loaded with calcium phosphates for dental pulp tissue regeneration. Iran J Chem Chem Eng 2025;44:1-16.
68. Attaeyan,A , Shahgholi,M and Khandan A. Fabrication and Characterization of Novel 3D Porous Titanium-6Al-4V Scaffold for Orthopedic Application Using Selective Laser Melting Technique. Iranian Journal of Chemistry and Chemical Engineering, 2024;43:66-82. doi: 10.30492/

ijcce.2023.1991010.5905.
69. Ghanbari N , Kamyab Moghadas B, Samadi F, Khandan A. FEM Analysis and Characterization of PVP-CMC-Forsterite Nano Composite Scaffolds via SLM 3D Printing for Bone Tissue Engineering. Iranian Journal of Chemistry and Chemical Engineering, 2025;44:3138-52. doi: 10.30492/ijcce.2025.2064498.7175.
70. Barbaz-Isfahani R, Jamali M, Pourkhamisi N, Khademi A, Iranmanesh P, Torabinia N, Khandan A. Comparative Analysis of Ceramic Nanoparticle Properties for Biomaterials: Implications for Applications and Material Selection Using Statistical Analysis. Nanochemistry Research 2026;11:133-51. doi: 10.22036/ncr.2025.523359.1478.
71. Barbaz-Isfahani R, Shahbaz A, Jamali M, Khademi A, Iranmanesh F, Iranmanesh, P, *et al*. Advanced bioprinting methodologies: A quantitative analysis and exploration of innovative techniques for tissue engineering. Nanomed Res J 2025;10:95-113.
72. Vakili N, Asefnejad A, Mohammadi M, Rezaei H, Khandan A. Improving physicochemical, mechanical, and biological properties of a porous polyvinyl alcohol/chitosan matrix via modification with magnesium and silicon agents. Nanomedicine Journal 2025;12:507-17. doi: 10.22038/nmj.2025.79321.1951.
73. Barbaz Isfahani R, Shahbaz A, Khademi A, Iranmanesh P, Khandan A, Sheikhbahaei E. Mechanical and chemical behaviour of nanoparticles in multicomponent dressings: Promoting wound healing with novel materials, intelligent monitoring, and enhanced healing outcomes. Nanochemistry Res 2025;10:482-515.
74. Mirmohammadi H, Fatalla AA, Razi A, Iranmanesh P, Khandan A, Barbaz-Isfahani R, *et al*. Enhancing the role of AI in the development of biomaterials through interdisciplinary collaboration. Dent Hypotheses 2025;16:57-8.
75. Khademi A, Khandan A, Iranmanesh P. Hydrogels for dental pulp repair: enhancing physicochemical and regenerative potential with CaP-loaded alginate-gelatin hydrogel scaffolds: a FEM and ANN modeling. Nanomedicine Journal 2026;13:183-95. doi: 10.22038/nmj.2025.84229.2115.
76. Khademi A, Khalifehzadeh S, Khandan A. Advancements in Diagnosing and Treating External Invasive Cervical Resorption: A Comprehensive Study on Biocompatible Materials and Finite Element Analysis. Iranian Journal of Chemistry and Chemical Engineering 2026;45:478-93. doi: 10.30492/ijcce.2025.2064546.7176.